PHYSICAL REVIEW C VOLUME 25, NUMBER 2 FEBRUARY 1982

Snowball model for light fragment production

David H. Boal and Mehr Soroushian
Theoretical Science Institute, Department of Chemistry, Simon Fraser University, Burnaby, British Columbia, Canada V5A 1S6

(Received 24 March 1981)

The snowball model for proton and electron induced light fragment production is investigated in some detail. The model involves a single scattering of the projectile, and multiple scatterings of the struck nucleon to form the observed fragment. The parameters of the model are examined and compared with qualitative estimates obtained by different methods. Predictions are made for electron induced fragment production.

[NUCLEAR REACTIONS Snowball model for inclusive production of light fragments; electron and proton induced reactions.]

I. INTRODUCTION

In the study of the emission of light fragments, the coalescence approach, in which energetic nucleons coalesce near the nuclear surface to form the observed fragment, has been in use for some time.[1,2] In order to say anything meaningful about the magnitudes of the cross sections in these reactions, however, one must know the details of the mechanism for producing these energetic nucleons. Many of the applications of the coalescence approach have come in heavy ion reactions.[3–6] There, it is often assumed that some excited nucleus is produced in the reaction, and that its nucleons have come to thermal equilibrium. Unfortunately, calculating the production cross section for this excited system is difficult, and so the normalization of these models has not been well tested. Where available, fits have been made to data for a few isotopically separated fragments. These fits involve a parameter which is a measure of the size of the phase space volume into which a nucleon can be emitted and coalesce to form a fragment. The value of the maximum allowable relative momentum p_0 is reasonably constant from fragment to fragment. This is not too surprising, because the expressions for the cross section involve raising p_0 to a large power, namely $3(A_F-1)$, where A_F is the number of nucleons in the fragment. Hence, a given change in the cross section will result in a much smaller change in p_0.

Recently,[7] we reviewed the existing data for electron and proton induced emission of energetic light fragments, in an effort to find simpler dynamics than that found in heavy ion reactions. Our conclusion, based heavily on the ratio of the (e,α) to (p,α) differential cross sections,[8,9] was that the most likely model for electron and proton induced fragmentation was one which involved a single scattering of the projectile followed by multiple scatterings of the struck nucleon as it loses its energy and forms the observed fragment. The cross section expressions for this model have both similarities and differences compared with those of the heavy ion coalescence models. Our purpose here will be to investigate this model, which we have called the snowball model, in more detail than was possible in our preliminary communication, in particular, looking at the questions of normalization and interpretation of parameters. Rather than try to fit data sets (for each fragment) separately, which tends to obscure the dependence of the cross sections on the parameters, we will make some simplifying assumptions which show the dependence fairly clearly. With the parameters so determined, predictions will then be made for electron induced fragmentation reactions, as a test of the model.

II. DETAILS OF THE MODEL

In the snowball model for proton induced reactions, the projectile first undergoes a single scattering on an off-shell nucleon in the nucleus, the struck nucleon being given an energy equal to the kinetic energy of the emitted fragment, T_q, plus an energy E^* of the residual system. Thus, as a consequence of the first scattering, the differential cross section $d^2\sigma/d\Omega\,dE$ for the emitted fragment

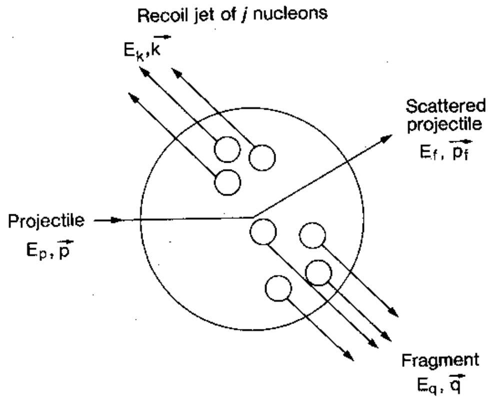

FIG. 1. Kinematic labels for snowball model. There are $A_T - A_F - j$ spectator nucleons.

is proportional to $d^2\sigma/d\Omega\, dE$ for the (p,N') reaction evaluated at the same incident proton energy E_p and at the same angle as that of the emitted fragment, on the average. Because of the lack of information on inclusive neutron production, we will assume that the (p,n) cross section for energetic neutron emission is equal to the (p,p') cross section.[10-18] The kinematic labels for the model are given in Fig. 1.

Both the mean multiplicity and the average number of collisions of a proton crossing a medium mass nucleus are roughly equal for projectiles in the 50–100 MeV range, the energy range of interest here for the first struck nucleon. Hence, we will assume that there is one nucleon emitted per NN collision in the nucleus.

Then, in subsequent scatterings of the primary struck nucleon, the probability that the ith struck secondary nucleon will scatter into a momentum space volume V_s about the average momentum per nucleon $\vec{q}/A_F$ is given approximately by

$$\frac{1}{\overline{M}}\frac{1}{\sigma_R}\int_{V_s}\frac{d^3\sigma(p,N')}{d^3p_i}d^3p_i \ , \tag{1}$$

where $\overline{M}$ is the mean nucleon multiplicity, σ_R is the reaction cross section and both cross sections are evaluated at an incident energy of T_q. Because the momentum of the ith nucleon is, on the average, collinear with the primary nucleon, we need to be concerned mainly with the behavior of $d^3\sigma/d^3p$ in (1) at forward angles and energies not close to the energy of the primary nucleon. Fortunately, this differential cross section is roughly constant at forward angles, and so we will extract it from the integral. The momentum space integral is then approximated at these nonrelativistic energies (for the fragment) by

$$V_s = \frac{4\pi}{3}p_s^3 \ , \tag{2}$$

where p_s is a parameter of the model. Clearly, p_s is closely related to the Fermi momentum of the nucleons in the emitted fragment. At this point, Pauli blocking will not be included, and so the p_s determined phenomenologically will be smaller than the Fermi momenta typical of light nuclei (about[19] 170 MeV/c for ^{6}Li, 221 MeV/c for ^{12}C). For our purposes, we will assume that p_s is the same for all of the light fragments considered here. Because the fragment nucleons "condense" around the primary struck nucleon, the volume in which the fragment forms is limited and the effect of spatial correlations should be small.

Lastly, we should include a combinatoric factor to evaluate what fraction of the emitted A_F nucleons have the appropriate number of protons and neutrons. This is given by

$$C_{FT} = \frac{Z_T!N_T!A_F!(A_T-A_F)!}{N_F!(N_T-N_F)!Z_F!(Z_T-Z_F)!A_T!} \ , \tag{3}$$

where the T and F subscripts refer to the target and fragment, respectively.

Hence, the cross section has the form

$$\frac{d^2\sigma(p,\text{fragment})}{d\Omega_q dE_q} = C_{FT}\frac{d^2\sigma(p,N')}{d\Omega\, dE}\left[\frac{1}{\overline{M}}\frac{1}{\sigma_R}\frac{d^3\sigma(p,N')}{d^3p}V_s\right]^{A_F-1} . \tag{4}$$

Before we pursue the consequences of this model further, there are several comments which should be made. Because of the small value of $\overline{M}$ compared to heavy ion reactions, we should fold in a distribution of multiplicities times a combinatoric factor for extracting $A_F - 1$ nucleons from each value of the multiplicity. Sample calculations show this effect to be of order unity, so we have omitted it. Also, as was indicated above, we have neglected Pauli blocking and detailed binding energy effects.

Lastly, the average momentum per nucleon of mass M for a nonrelativistic fragment with kinetic energy T is given by

$$\frac{q}{A_F}=\left[\frac{2MT}{A_F}\right]^{1/2}. \tag{5}$$

At fixed T, the average momentum per nucleon will fall with increasing A_F until it is less than p_s. At these large values of A_F, one should observe a saturation effect wherein after the first n collisions, a significant number of any further scatterings all result in more nucleons being added to the developing cluster.

Because of the rough constancy of the terms in the square brackets in Eq. (4) over the range of energies per nucleon involved in light fragment formation for varying A_F, a plot of the logarithm of C_{FT}^{-1} times the fragment differential cross section vs A_F-1 should yield a straight line whose slope is the logarithm of the square brackets. An example of this kind of plot is shown on Fig. 2 for $T_p=480$ MeV, $T_q=50$ MeV, and $\theta_q = 90°$. The data points are from a smooth curve fit to the data in Ref. 20. The saturation effect discussed above is clearly visible at $A_F \approx 9$, which corresponds to an average momentum per nucleon of about 100 MeV/c. We therefore expect p_s to be in the 100–180 MeV/c range.

To extract p_s from the slope of such plots, we used average values[3] for $(1/A_T)d^2\sigma/d\Omega\,dE$ for (p,p') at bombarding energies of 50–100 MeV (the energies appropriate for the secondary scatterings), and at forward angles, of 60 μb/MeV sr nucleon, for $(1/A_T)\sigma_R$ the value[3] of 13 mb/nucleon, and for $\overline{M}$ a value of 3. (A_T is the mass number of the target.) The values of p_s obtained from a least squares fit to data[20–25] for stable isobars with $3 \le A_F \le 9$ are shown in Table I as calculation I. These numbers cannot be directly equated with the average Fermi momemta of light nuclei, since Pauli blocking has been ignored. Indeed, the numbers are lower than the value for the Fermi momentum of 170 MeV/c obtained[19] for ^{6}Li and 221 MeV/c for ^{12}C in a Fermi gas model analysis of inelastic electron scattering in the quasifree region. (This analysis gave the expected 250–265 MeV/c result for nuclei with 40 or more nucleons.) The values of p_s correspond more closely to the average momentum of the nucleons in the nucleus, which we would expect to be about 150 MeV/c for a Fermi gas with a maximum momentum of 200 MeV/c.

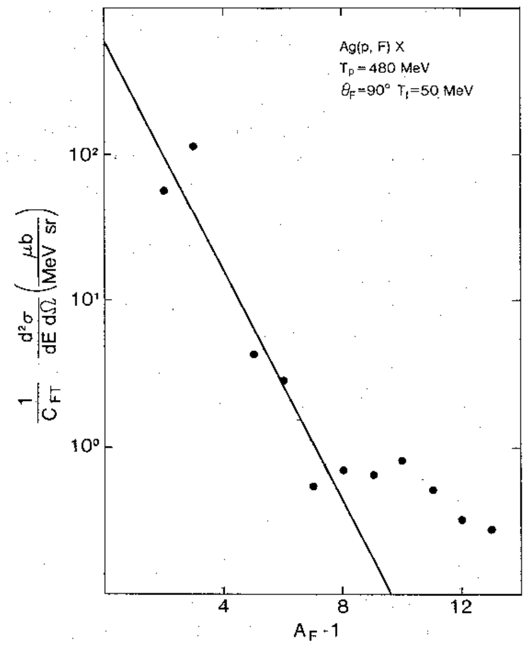

FIG. 2. Logarithmic plot of $C_{FT}-1 \cdot d^2\sigma/d\Omega\,dE$ vs A_F-1 for fragments emitted at 90° and 50 MeV under bombardment of 480 MeV protons. The points are from a smooth fit to the data of Ref. 20.

TABLE I. Calculation of p_s with (II) and without (I) Pauli blocking for various energy and angle combinations.

Target	Projectile energy (MeV)	Fragment angle	Fragment energy (MeV)	Calculated p_s I	(MeV/c) II
Ag	480	90°	50	155	197
Ag	480	90°	100	157	198
Ag	480	160°	50	151	192
Ag	480	160°	100	156	198
Ag	5500	90°	50	166	212
Ag	5500	90°	100	172	219
U	5500	90°	50	179	228
U	5500	90°	100	182	232

The magnitude and sign of the corrections to p_s which would be made by inclusion of Pauli blocking can be estimated by the following crude calculation. This approach is at best an approximation for heavy systems, and is certainly not put forward here as an accurate calculation for light systems, but should, nevertheless, indicate the magnitude of corrections expected.

Our calculation goes as follows: After the first nucleon has been scattered into the phase space volume V_s, part of that volume will not be available to the second nucleon. Let us assume that the first i nucleons are scattered into their lowest energy configurations. The density of states for the fragment is given by

$$d\eta = \frac{16\pi\left[\frac{4}{3}\pi r_0{}^3 A_F\right]}{h^3} p^2 dp \ , \tag{6}$$

with r_0 taken to be 1.2 fm. Integrating this expression, and setting the left-hand side (lhs) equal to A_i, gives a corresponding momentum p_i from the right-hand side (rhs) up to which the nucleon energy levels are filled:

$$p_i = p_F\left[\frac{A_i}{A_F}\right]^{1/3} \tag{7}$$

Therefore, the allowed volume into which the ith nucleon can scatter is $V_s[1-(A_i-1)/A_F]$. Hence, the $V_s^{A_F-1}$ part of Eq. (4) should be multiplied by B_F, where

$$B_F = \left[1-\frac{1}{A_F}\right]\left[1-\frac{2}{A_F}\right]\cdots\left[1-\frac{A_F-2}{A_F}\right] = \frac{A_F!}{A_F^{A_F-1}} \ . \tag{8}$$

We can proceed as before to calculate p_s by plotting $\log[(C_{FT}B_F)^{-1}\,d^2\sigma/d\Omega\,dE]$ vs A_F-1. An example of this is shown in Fig. 3. The calculated values of p_s from this analysis are shown in column II of Table I. It is clear that the numbers are much closer to what one would expect on the basis of the electron data. We will not use this Pauli blocking factor any further in these calculations.

III. GEOMETRICAL EFFECTS

Returning to Fig. 2, the y intercept should be equal to about twice the Ag$(p,p')X$ cross section. In fact, the intercept from the fit to the fragment data is about $\frac{2}{3}$ of this number, with the average for the other angle and energy combinations listed in Table I being somewhat less than one half the free (p,p') cross section times two. Part of this discrepancy may originate in the assumption that the (p,n) cross sections are the same as the (p,p'). Part may also be attributable to the fact that the residual nucleus in the fragmentation reaction may be left with more excitation energy than in the (p,p') reaction, so that the intercept should be compared with the (p,p') reaction at higher $T_{p'}$. If one takes this approach, an excitation energy in the 30 MeV range would be required to explain the discrepancy.

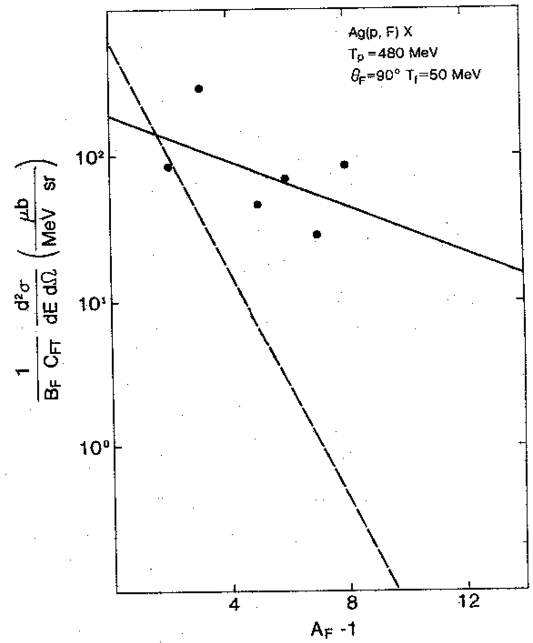

FIG. 3. Logarithmic plot of $(B_F C_{FT})^{-1} d^2\sigma/d\Omega\,dE$ vs A_F-1 for the same conditions as in Fig. 2. The dashed line is the fit from Fig. 2.

While this is not unreasonable, the target dependence argues that the effect may have, at least in part, a geometrical origin. As a function of A_T, the alpha production cross section per target nucleon is roughly constant for A_T in the 100 range, but drops off for light targets. In contrast, at these projectile and ejectile energies, the cross section per target nucleon for the (p,p') reaction is fairly constant from Li to Ta. This suggests that, while most target nucleons contribute to the cross section for the (p,p') reaction, only those nucleons sufficiently far away from the nuclear surface to be able to undergo enough collisions to form a fragment will contribute to the fragmentation cross section.

To pursue this idea further and obtain a qualitative estimate of the minimum distance from the nuclear surface ($\equiv D$) involved, we perform the following calculation: Let us assume that the nucleus is of uniform density ρ, with a sharp edge at $R = 1.2\, A^{1/3}$ fm. Then the number of nucleons per unit area as seen along the fragment direction (at a distance b from the center of the nucleus perpendicular to the fragment direction) which are greater than a distance D from the surface is

$$\begin{aligned}&\rho[2(R^2-b^2)^{1/2}-D],\ \text{if } b<(R^2-D^2/4)^{1/2}\\&0,\ \text{if } b>(R^2-D^2/4)^{1/2}\end{aligned} \tag{9}$$

Integrating over the surface area perpendicular to the fragment direction, we find that the total number of nucleons satisfying this constraint is

$$A_{\text{eff}} = A_T[1+\tfrac{1}{2}(\xi^3-3\xi)]\ , \tag{10}$$

where

$$\xi = D/2R\ . \tag{11}$$

A rough estimate for the value of D can be obtained from the ratio of twice the (p,p') cross section to the intercept of the log $(C_{FT}{}^{-2}\, d^2\sigma/d\Omega\, dE)$ plot. If only about half the target nucleons for a silver target are available to the primary interaction in fragment formation, then D must be around 4 fm.

A better way of determining D is to look at the target dependence of the cross section. Because the greatest amount of data for different targets has been collected for α emission, we will concentrate on the (p,α) and (e,α) reactions. Unfortunately, not all target data are available at the same energies and angles, so some corrections will have to be made to allow for meaningful comparisons. First we will look at the data around 5 GeV incident proton energy.

For bombarding energies in the 500–800 MeV range, the differential cross sections per target nucleon for the (p,p') reaction with ejectiles in the 50–100 MeV range are roughly constant as we stated above. However, for bombarding energies in the 5 GeV region, both proton and fragment production cross sections per target nucleon show at least a factor of 4 increase in going from light to heavy targets. Hence, we must divide the fragment cross sections by the (p,p') cross sections so that the only A_T dependence on the rhs of the equation

$$\frac{d^2\sigma}{d\Omega\, dE}(p,F)\Big/ C_{TF}\frac{d^2\sigma}{d\Omega\, dE}(p,N') = G_F B_F\left[\frac{1}{\bar{M}}\frac{1}{\sigma_R}\frac{d^3\sigma(p,N')}{d^3p}V_s\right]^{A_F-1} \tag{12}$$

is in G_F, where

$$G_F \equiv 1+\tfrac{1}{2}[\xi^3-3\xi]\ . \tag{13}$$

In Fig. 4, the fragment cross sections[22,23,25] at 4.9 GeV and 90° have been divided by C_{FT} times the (p,p') cross sections[16] at 5.14 GeV and 160° (the nearest comparable data) interpolated to the appropriate target. In addition, the carbon target (p,α) data was taken at 2.1 GeV, and so a correction factor from the estimated 2.1 and 4.9 GeV (p,p') cross sections has been applied. Lastly, the data have been normalized to a uranium target to avoid having to estimate the 90° to 160° ratio of the (p,p') cross sections. One can see that the three data points (since the uranium is then defined as unity) agree well with Eq. (13) for $D = 4$ fm, in good agreement with that obtained from the intercept argument.

At the low bombarding energy of 100 MeV fewer corrections are required to the existing data, but the cross sections are more sensitive to the Q values of the reaction. This may be of importance because the Q values change by about 10 MeV in going from light to heavy targets. Depending on how one splits the extra energy released between the observed fragment and the residual system, the energies at which the cross sections should be compared could change, giving a corresponding change in cross sections by as much as a factor of 2. For these low energy reactions, then, we will look at a more limited target range for which the Q values do not vary as much. Hence, the comparisons are made for light nuclei and are normalized to a target of about 100 nucleons [90 for (p,α) (Ref. 9) and 94 for (e,α) (Ref. 8)]. A fit has not been attempted, but rather the curve is shown for $D = 4$ fm. Again, this agrees with the intercept argument (based on substantially less fragment data) that only about half the number of target nucleons are available for fragment formation at these energies.

In the comparisons shown in Figs. 4 and 5, error bars have been omitted because we have not been able to compute them systematically. They are generally at the 15% level.

IV. ELECTRON INDUCED REACTIONS

Data for electromagnetically induced fragment emission for fragment kinetic energies greater than 30 MeV are quite sparce, and so the kind of analysis used in Sec. II is not applicable at the present time. Rather, we will use the p_s and D

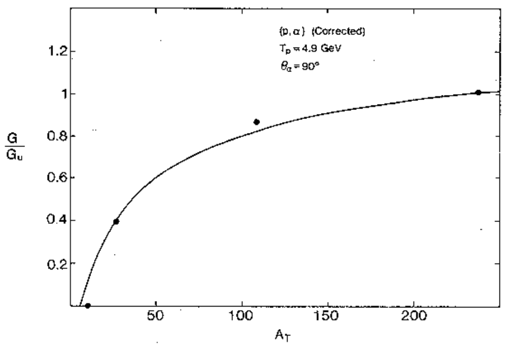

FIG. 4. Ratio of G for a given target to G for uranium, as a function of A_T for the (p,α) reaction. The data were taken at 4.9 GeV and 90°, except for the carbon datum which was taken at 2.1 GeV and scaled here by the estimated ratio of (p,p') cross sections at the appropriate energies. Data from Refs. 22, 23, and 25.

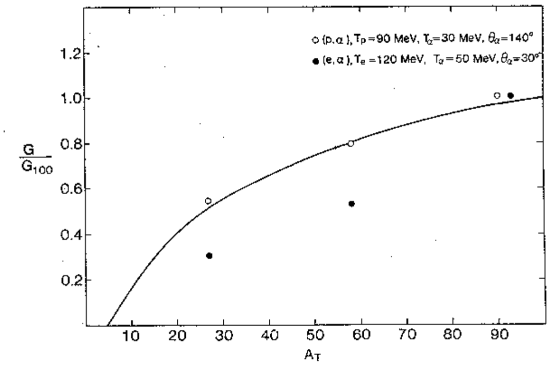

FIG. 5. Ratio of G for a given target to G at $A_T = 100$ (solid curve). The data points were normalized to $A_T = 90$ [(p,α) reaction, Ref. 9] or 94 [(e,α) reaction, Ref. 8].

values found in the previous sections, along with a model calculation of the (e,p) reaction, to predict the $(e$, fragment) cross sections. These will be compared with data, where available.

In a previous paper[26] coauthored by one of us, a direct knockout model for the (p,p') reaction[27] was refined and extended to photon and electron induced reactions.[28] We will use this model, suitably modified, to predict the (e,p) cross sections. In the model, a proton moving with momentum $-\vec{k}$ is struck by the incident electron, the proton's momentum changing to $\vec{q}$. The particle or particles recoiling against the proton with momentum $\vec{k}$ are then assumed to escape from the nucleus, as is the electron, with no further interactions with the struck proton. A sum is performed over the number of nucleons, j, in the recoiling jet, each jet having an invariant mass distribution $D_j(K)$ of the form

$$D_j(K) = \frac{j}{2\sqrt{\pi}\eta_j \mathcal{M}_j(K)} \times \exp\left\{-\left[\frac{\mathcal{M}_j(K) - \mathcal{M}_j^0}{\eta_j}\right]^2\right\}, \tag{14}$$

where $\mathcal{M}_j$ is the invariant mass of the j nucleon jet (of four-momentum K), and η_j is equal to j times 15 MeV. The distribution is centered at $\mathcal{M}_j^0$, which we have chosen to be j times the free nucleon mass. For a single nucleon recoiling, there is, of course, no invariant mass distribution, and so an energy of 10 MeV has been added to the proton to approximate the excitation energy of the spectators. Otherwise, the excitation energy of the spectator system has not been treated separately, but rather is assumed to be bound up in $D(K)$. The differential cross section then has the form

$$\frac{d^2\sigma}{d\Omega_q dE_q} = \frac{1}{2^4(2\pi)^5} \cdot 4m_e^2 \frac{q}{p} \sum_{j=1}^{A_T-1} \frac{a_j(j+1)}{M_{T_j}} \int \frac{d^3p_f}{E_f} dE_k D_j(K) n(k) \,|\, T_{ep} \,|^2 \delta(\text{energy}) . \tag{15}$$

The vertex function $n(k)$ would be interpreted as the single particle momentum distribution in the plane wave impulse approximation, and is parametrized by

$$n(k) = C\left[2\cosh\left[\frac{k}{2k_0}\right]\right]^{-2} \equiv C\, F(k) . \tag{16}$$

The constant k_0 was determined by fitting the (p,p') data to have a value of 120 MeV/c, and the constant C is determined by the approximate normalization condition

$$Z_T = \frac{C \int F(k) d^3k \sum_{i=1}^{A_T - 1} a_i}{2(2\pi)^3 M_B}, \tag{17}$$

where M_B is the average bound nucleon mass, taken to be 931.5 MeV. The weighting factors a_j are simply taken to be

$$a_j = g^{j-1}, \tag{18}$$

and g is found to be 0.9 in a simultaneous fit with k_0.

The interaction between the electron and the proton is given by the on-shell expression for $|T_{ep}|^2$. When this is integrated out by means of the forward peaking approximation, the expression for the differential cross section becomes

$$\frac{d^2\sigma}{d\Omega_q dE_q} = \frac{C}{(4\pi)^2} |F_p|^2 \alpha_{em}{}^2 (\hbar c)^2 F(k) \frac{q}{\mathrm{PSP}} \sum_{j=1}^{A_T - 1} \frac{a_j . j . (j+1)}{M_{T_j}} \int \frac{d\mathscr{M}_k}{E_k} \left\{ \frac{\exp\{-[(\mathscr{M}_k - \mathscr{M}_k^0)/\eta_j]^2\}}{\sqrt{\pi}\eta_j} \right\} \frac{p_f}{p_i} \mathrm{INT}, \tag{19}$$

where i (f) is the initial (final) electron state, and where the integral INT is approximately

$$\mathrm{INT} = \frac{1}{E_i E_f} \left\{ \left[2q^2 \sin^2\theta_q \frac{E_i{}^2 + E_f{}^2}{(E_i - E_f)^2} + (1+\kappa)^2 (E_i{}^2 + E_f{}^2) \right] \ln \left[\frac{2E_i E_f}{m_e (E_i - E_f)} \right] - 2E_i E_f \left[\frac{2q^2 \sin^2\theta_q}{(E_i - E_f)^2} + (1+\kappa)^2 \right] \right\}, \tag{20}$$

and where the phase space factor PSP is

$$\mathrm{PSP} = \left| p_f \left[\frac{1}{E_f} + \frac{1}{E_k} \right] + \frac{1}{E_k} (q \cos\theta_q - p_i) \right|, \tag{21}$$

the quantity κ having a value of 1.79.

In both Eqs. (17) and (19) it is assumed that the electron only interacts with protons. This may be an oversimplification if the interaction of the virtual photon is with a p-n pair which allows either or both nucleons to be put on the mass shell. This assumption cannot be directly tested by the relative magnitudes of the (γ,n) vs (γ,p) reactions, for example, since secondary charge exchange reactions have not been included here.

As a first test of these calculations, we have applied them to the (e,α) data at 120 MeV electron energy. Shown in Fig. 6 is the differential cross section per target nucleon on Ni and Au targets at fixed alpha kinetic energy as a function of angle as given by Eq. (19) and

$$\frac{d^2\sigma}{d\Omega\, dE}(e,F) = G_F C_{FT} \frac{d^2\sigma}{d\Omega\, dE}(e,p) \times \left[\frac{1}{\bar{M}} \frac{1}{\sigma_R} \frac{d^3\sigma(p,N')}{d^3p} V_s \right]^{A_F - 1} \tag{22}$$

with p_s = 155 MeV/c and D=4 fm. The nearly identical predictions for Ni and Au are coincidental, and involve cancellation of terms which vary by about 30% between targets. These predictions are not accurate to better than a factor of 2, given the assumption that there are only primary e-p reactions and the omission of binding energy considerations. Furthermore, while the geometrical factor introduced in Sec. III seems to describe the (p,α) target dependence well, its description of the (e,α) target dependence is not so good and so an additional discrepancy of up to 40% can be expected.

Comparison with data of the predicted cross section for a given fragment is not the only test of the model. Better tests would involve comparative analyses of several fragment types, as outlined in Sec. II. For example, shown in Fig. 7 is the predicted energy dependence for Ag(e,F)X for $3 \le A_F \le 9$ with the fragment emitted at 90° and 50 MeV kinetic energy. Similarly, in Fig. 8 is the energy spectrum of the fragments expected at 90° for an electron kinetic energy of 250 MeV.

V. CONCLUSION

We have described a model for energetic light fragment production in proton and electron in-

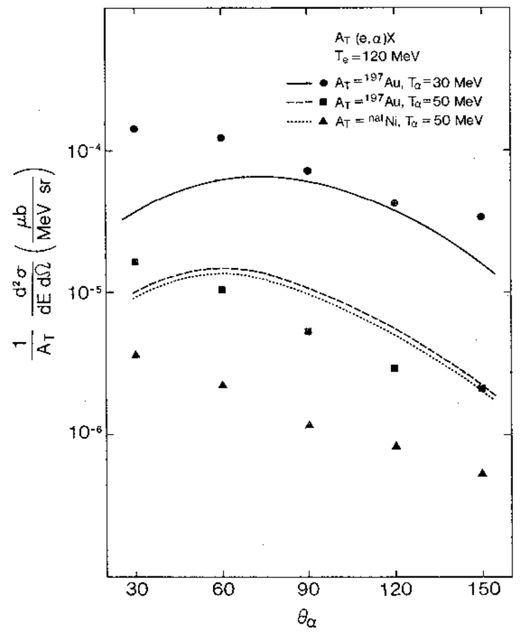

FIG. 6. Comparison of the snowball model predictions with data for the (e,α) reaction. The incident electron energy is 120 MeV, while the target and observed alpha particle energies are: ^{197}Au, 30 MeV (solid curve, circles); ^{197}Au, 50 MeV (dashed curve, squares); and ^{nat}Ni, 50 MeV (dotted curve, triangles).

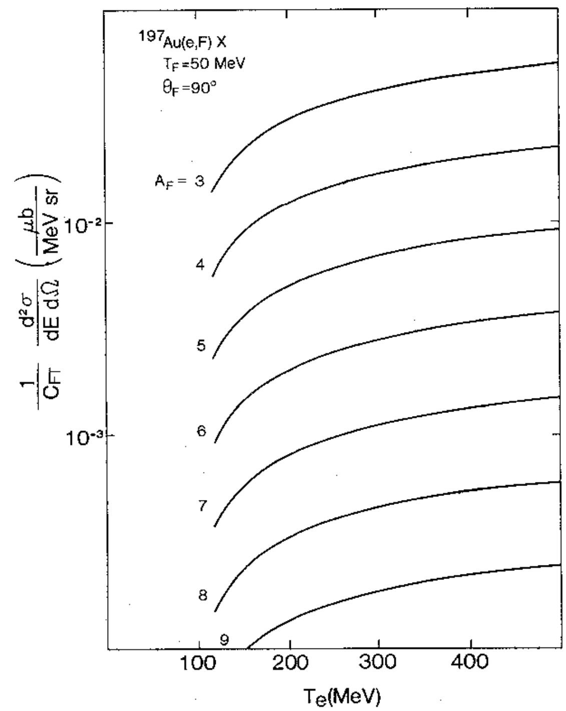

FIG. 7. Predicted projectile energy dependence of the Ag$(e,F)X$ reaction for $3 \le A_F, \le 9$ with the fragment emitted at 90° and 50 MeV.

duced reactions at intermediate energy. There are two parameters associated with this model: p_s, which determines the volume of phase space into which a secondary struck nucleon can scatter and become part of a fragment, and D, an "accumulation length" which is a measure of the average distance away from the nuclear surface that the primary struck nucleon must be in order to form a fragment.

The value of p_s determined by analyzing the data without including Pauli blocking is in the 150–170 MeV/c range, comparable to what one would expect for the average momentum of the nucleons in a light nucleus treated as a Fermi gas. Inclusion of a coarse estimate of the effects of Pauli blocking raises p_s to the 200–220 MeV/c range, again comparable to the estimated Fermi momentum of a light nucleus. Because of its crudity, the Pauli blocking calculation is probably not of great use in predicting cross sections, and is only introduced here to get an estimate of the blocking effect.

The parameter D is estimated by two means. One is an estimate of the effective number of target nucleons available for fragment formation in a silver target, which yields a value of about 4 fm. Similarly, the variation of a particular (p,F) reaction with A_T also yields a value of about 4 fm. While it is difficult to give a meaningful prediction for this number, it is certainly observed to be in the range one would expect for the pickup of a few nucleons.

One factor which has been left out of these calculations is the effect of binding energy. The variation in binding energy per nucleon for the stable nuclides discussed here will result in a small variation of p_s. However, because p_s is being raised to the $3(A_F-1)$ power in these calculations, changes in p_s of 5%, for example, can easily result in changes of a factor of 2 in the cross section. Model predictions for p_s to this accuracy are beyond the scope of the present calculation. Binding energy effects may also be responsible for the increase in p_s in going from an Ag to U target at 5.5 GeV incident energy. The Q values for emitting a mass 9 fragment, for example, from a U target will be larger than for an Ag target, and hence a larger value of p_s would be extracted using the analysis presented above.

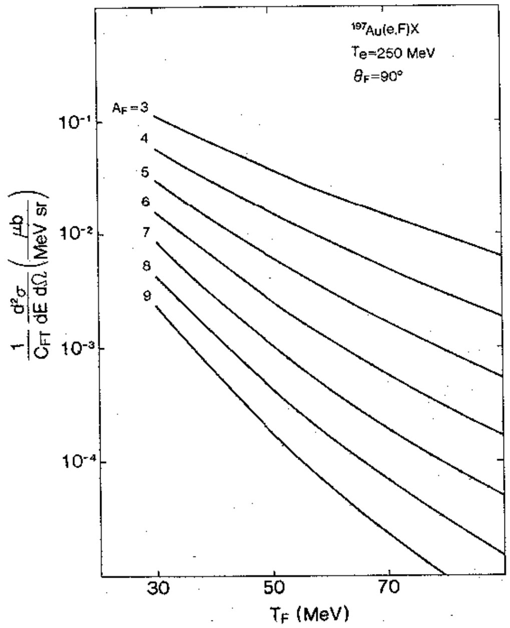

FIG. 8. Predicted energy spectrum of fragments emitted at 90° under a bombarding energy of 250 MeV in the Ag$(e,F)X$ reaction.

Lastly, estimates were made for the (e,F) reactions with $3 \leq A_F \leq 9$. These calculations are not accurate to better than a factor of 2, but do indicate the trends expected as a function of projectile and fragment energy, angle, and mass number. Measurement of these reactions should provide a good test of the model. Another good test would involve the (γ,F) reactions, particularly with tagged photons. We have made absolutely normalized predictions for these electron induced reactions on the basis of parameters determined from proton induced reactions. Because of the pivotal role played by the (e,p) reaction, which we have had to calculate here, its measurement (with a variety of targets) would help to resolve the target dependence discrepancy in the (e,α) reaction, which may arise from: (i) improperly calculated (e,p) cross section, (ii) excitation energies and Q values playing a more important role than at higher energies, and (iii) projectile and target dependent multiple scattering.

ACKNOWLEDGMENTS

The authors would like to thank R. G. Korteling and R. E. L. Green of Simon Fraser University for providing them with unpublished data. We also wish to thank R. Woloshyn (TRIUMF) for several stimulating discussions. Lastly, one of us (D. H. B.) expresses his gratitude to the Natural Sciences and Engineering Research Council for financial support.

[1]S. T. Butler and C. A. Pearson, Phys. Rev. 129, 836 (1963).
[2]A. Schwarzschild and Č. Zupančič, Phys. Rev. 129, 854 (1963).
[3]H. Machner, Phys. Lett. 86B, 129 (1979).
[4]H. H. Gutbrod *et al.*, Phys. Rev. Lett. 37, 667 (1976).
[5]M.-C. Lemaire, Phys. Lett. 85B, 38 (1979).
[6]A. Mekjian , Phys. Lett. 89B, 177 (1980); J. I. Kapusta, Phys. Rev. C 21, 1301 (1980).
[7]D. H. Boal, R. E. L. Green, R. G. Korteling, and M. Soroushian, Phys. Rev. C 23, 2788 (1981).
[8]A. G. Flowers *et al.*, Phys. Rev. Lett. 40, 709 (1978); 43, 323 (1979).
[9]J. R. Wu, C. C. Chang, and H. D. Holmgren, Phys. Rev. C 19, 698 (1979).
[10]D. M. Corley *et al.*, Nucl. Phys. A184, 437 (1972).
[11]S. Frankel *et al.*, Phys. Rev. Lett. 36, 642 (1976).
[12]S. Frankel *et al.*, Phys. Rev. C 18, 1375 (1978).
[13]S. Frankel *et al.*, Phys. Rev. Lett. 41, 148 (1978).
[14]V. I. Komarov *et al.*, Nucl. Phys. A326, 297 (1979).
[15]V. I. Komarov *et al.*, Phys. Lett. 69B, 37 (1977); 80B, 30 (1978).
[16]N. A. Burgov *et al.*, Yad. Fiz. 30, 720 (1979) [Sov. J. Nucl. Phys. 30, 371 (1979)].
[17]G. Roy *et al.*, Phys. Rev. C 23, 1671 (1981).
[18]Y. D. Bayukov *et al.*, Phys. Rev. C 20, 764 (1979).
[19]R. R. Whitney *et al.*, Phys. Rev. C 9, 2230 (1974).
[20]R. E. L. Green and R. G. Korteling, Phys. Rev. C 18, 311 (1978); 22, 1594 (1980).
[21]R. E. L. Green, K. P. Jackson, and R. G. Korteling (unpublished).
[22]A. M. Poskanzer, G. W. Butler, and E. K. Hyde, Phys. Rev. C 3, 882 (1971).
[23]E. K. Hyde, G. W. Butler, and A. M. Poskanzer, Phys. Rev. C 4, 1759 (1971).
[24]R. G. Korteling, C. R. Toren, and E. K. Hyde, Phys. Rev. C 7, 1611 (1973).
[25]G. D. Westfall *et al.*, Phys. Rev. C 17, 1368 (1978).
[26]D. H. Boal and R. M. Woloshyn, Phys. Rev. C 23, 1206 (1981).
[27]R. D. Amado and R. M. Woloshyn, Phys. Rev. Lett. 36, 1435 (1976).
[28]These reactions had also been looked at by G. L. Vysotskii and A. V. Vysotskaya, Yad. Fiz. 9, 1177 (1969) [Sov. J. Nucl. Phys. 9, 689 (1969)].